cmgh
CELLULAR AND MOLECULAR GASTROENTEROLOGY AND HEPATOLOGY

ORIGINAL RESEARCH

Foxl1-Expressing Mesenchymal Cells Constitute the Intestinal Stem Cell Niche

Reina Aoki,[1,*] Michal Shoshkes-Carmel,[1,*] Nan Gao,[1] Soona Shin,[1] Catherine L. May,[1] Maria L. Golson,[1] Adam M. Zahm,[1] Michael Ray,[2] Caroline L. Wiser,[2] Christopher V. E. Wright,[2] and Klaus H. Kaestner[1]

[1]*Department of Genetics and Center for Molecular Studies in Digestive and Liver Diseases, Perelman School of Medicine, University of Pennsylvania, Philadelphia, Pennsylvania;* [2]*Vanderbilt University Program in Developmental Biology, Vanderbilt Center for Stem Cell Biology, Department of Cell and Developmental Biology, Vanderbilt University Medical Center, Nashville, Tennessee*

SUMMARY

Forkhead box l1+ cells are a small subset of mesenchymal subepithelial fibroblasts. These cells are a critical component of the intestinal stem cell niche as shown by using 2 separate models to ablate these cells.

BACKGROUND & AIMS: Intestinal epithelial stem cells that express leucine-rich repeat-containing G-protein coupled receptor 5 (Lgr5) and/or B cell specific Moloney murine leukemia virus integration site 1 (Bmi1) continuously replicate and generate differentiated cells throughout life. Previously, Paneth cells were suggested to constitute an epithelium-intrinsic niche that regulates the behavior of these stem cells. However, ablating Paneth cells has no effect on the maintenance of functional stem cells. Here, we show definitively that a small subset of mesenchymal subepithelial cells expressing the winged-helix transcription factor forkhead box l1 (Foxl1) are a critical component of the intestinal stem cell niche.

METHODS: We genetically ablated Foxl1+ mesenchymal cells in adult mice using 2 separate models by expressing either the human or simian diphtheria toxin receptor under Foxl1 promoter control.

CONCLUSIONS: Killing Foxl1+ cells by diphtheria toxin administration led to an abrupt cessation of proliferation of both epithelial stem- and transit-amplifying progenitor cell populations that was associated with a loss of active Wnt signaling to the intestinal epithelium. Therefore, Foxl1-expressing mesenchymal cells constitute the fundamental niche for intestinal stem cells. *(Cell Mol Gastroenterol Hepatol 2016;2:175–188; http://dx.doi.org/10.1016/j.jcmgh.2015.12.004)*

Keywords: Intestinal Stem Cell Niche; Wnt; Mesenchyme.

Adult multipotent stem cells replenish the gut epithelium both during homeostasis and after injury throughout life. The mammalian intestinal epithelium undergoes complete regeneration every 3–5 days; this renewal is supported by multipotent intestinal stem cells.[1–6] Epithelial stem cell populations reside in 2 zones: at the crypt base and at the +4 position, 4–6 cell widths above the crypt base. Cells in both zones express markers associated with stem cell behavior, such as CD24 and Lrig1.[4,5] In addition, there are zone-specific markers. For the small intestine, the crypt base cells are marked by leucine-rich repeat-containing G-protein coupled receptor 5 (Lgr5)[1] and Olfm4,[7] and the +4 position cells express Bmi-1, HopX, and mTert.[2,3,8] These epithelial stem cells divide to produce progenitor (or transit-amplifying) cells that proliferate rapidly and then differentiate into Paneth cells, which are located at the crypt base, or into goblet cells, enteroendocrine cells, M cells, and absorptive enterocytes that are located closer to the gut lumen.

Stem cell niches are defined as local microenvironments that provide physical support and/or molecular signals necessary for proper stem and progenitor cell replication and differentiation. Wnt signaling has been established as the major driver of intestinal stem and progenitor cell proliferation, as evidenced, for instance, by a rapid loss of proliferation when the secreted Wnt inhibitor Dickkopf-1 is overexpressed in the epithelium.[9,10] However, the cellular identity of the intestinal stem cell niche has remained controversial. Sato et al[11] concluded that epithelial Paneth cells constitute the niche for Lgr5+ stem cells in intestinal crypts, based on the fact that Paneth cells elaborate important signaling molecules such as Wnt3 and EGF and on the observation that in vitro organoid formation by Lgr5+ stem cells was enhanced by co-culture with a Paneth cell–enriched population. However, complete and permanent absence of Paneth cells in mice deficient for the

*Authors share co-first authorship.

Abbreviations used in this paper: **BAC, bacterial artificial chromosome; cDNA, complementary DNA; Foxl1, forkhead box l1; hDTR, human diphtheria toxin receptor; iDTR, inducible diphtheria toxin receptor; mRNA, messenger RNA; Myh11, rabbit myosin heavy chain 11; PBS, phosphate-buffered saline; PCR, polymerase chain reaction; YFP, yellow fluorescent protein.**

Most current article

2352-345X
http://dx.doi.org/10.1016/j.jcmgh.2015.12.004

transcription factor Math1 (Atoh1) had no impact on intestinal stem cell maintenance and proliferation.[12,13] The latter studies support earlier work by Garabedian et al[14] who used 2 independent methods to ablate mature Paneth cells and concluded that "stemness in the crypt is not defined by instructive interactions involving the Paneth cells." Moreover, epithelial-specific deletion of Wnt3 had no effect on intestinal stem cells in mice, suggesting the presence of other Wnt source(s).[15] These findings point to the existence of an extraepithelial source of Wnt and other signaling molecules necessary to maintain epithelial homeostasis.

Materials and Methods

Derivation of Forkhead Box l1–Human Diphtheria Toxin Receptor Mice

All protocols were approved by the Institutional Animal Care and Use Committee of the University of Pennsylvania. The human diphtheria toxin receptor (*hDTR)* coding sequence (NM_001945.1) was introduced into the coding region of the mouse forkhead box l1 (*Foxl1*) gene in the bacterial artificial chromosome (BAC) RP23-446J14 by means of BAC recombineering as described previously.[16] The targeting primers were as follows:

forward: GGGGCAAAGTCCTTAGGACTCCCCGGTGGAGCG GAGAGGCTGCTGTCGCCGAATTCGGCACGAGGGCTACGCGGG; reverse: AGGCCCCTCAGTGCACGACTTTGGCCGGCACGGGTAC GCTGCTCCAAACC AGCTCCACCGCGGTGGCGGCCGCTC.

The resulting *Foxl1–hDTR* BAC was linearized and microinjected into the pronucleus of C57Bl/6 mice. The positive transgenic founders were identified by genomic polymerase chain reaction (PCR) and crossed to C57Bl/6 mice for at least 5 generations. Animals were euthanized at 2–6 months of age for subsequent experiments.

Generation of Foxl1–Cre;Rosa–iDTR/YFP, Foxl1–Cre;Rosa–YFP, and Foxl1–Cre; Rosa–mT/mG Mice

Foxl1–Cre mice were generated and characterized previously.[16] *Foxl1–Cre* mice were crossed to *Rosa*–inducible diphteria toxin receptor (*iDTR*)/yellow fluorescent protein (*YFP*) mice (Jackson Laboratories, Bar Harbor, ME) to obtain *Foxl1–Cre;Rosa–iDTR/YFP* mice. *Foxl1–Cre;Rosa–*membrane-targeted dimer tomato protein (*mT*)/membrane-targeted green fluorescent protein (*mG*) mice, *Foxl1–Cre* mice resulted from crossing to *Rosa–mT/mG* mice (Jackson Laboratories). Animals were killed at 2–6 months of age for subsequent experiments.

Diphtheria Toxin Treatment

For *Foxl1–hDTR* mice, diphtheria toxin (Sigma-Aldrich, St. Louis, MO) dissolved in 0.9% sodium chloride was administered intraperitoneally at 20 ng/g body weight. Mice were injected on days 0 and 2 and killed on day 3. *Foxl1–Cre;Rosa–iDTR/YFP* mice and their control littermate (*Rosa–iDTR/YFP*) mice were administered diphtheria toxin at 22 ng/g body weight, twice daily from days 0–3, and killed on day 4.

Anti-Foxl1 Antibody Production

A Foxl1–pUC57 codon-optimized plasmid containing amino acids 150–255 of mouse Foxl1 (avoiding regions of similarity with other Fox proteins, especially focusing on non–winged-helix domains with good antigenicity prediction and likely subdomain folding) with flanking BamHI/HindIII sites was generated (GenScript USA, Inc, Santa Clara, CA). The BamHI/HindIII fragment was inserted into pGexKG,[17] confirmed by sequencing, and used to produce soluble GST-Foxl1 fusion protein from bacteria. GST-Foxl1 was dialyzed against phosphate-buffered saline (PBS) and used as an antigen in goat and guinea pig (SDIX, LLC) or chicken (Aves Labs). Raw sera/antibodies were used to purify Foxl1-specific antibodies via GST/*Escherichia coli*–extract depletion and GST-Foxl1 matrix-based affinity purification. GST-Foxl1 protein production and antibody purification were performed as described previously.[18]

Fluorescent Activated Cell Sorting, RNA Isolation, and Sequencing Library Preparation

Isolation of Foxl1+ cells using fluorescent-activated cell sorting was performed using *Foxl1–Cre;Rosa–YFP* mice. Small intestines were dissected and washed thoroughly with PBS. Intestinal villi were scraped using a coverslip and the remaining tissue was incubated in 30 mmol/L EDTA plus 1.5 mmol/L dithiothreitol and Hank's balanced salt solution on ice for 20 minutes and subsequently incubated in 30 mmol/L EDTA at 37° for 8 minutes to completely remove the epithelium. After vigorous washes, the remaining mesenchymal fraction was collected and cut into small pieces. The mesenchymal tissue was collected by centrifugation and resuspended in 7 mg/mL Dispase II/0.05% trypsin solution (Sigma-Aldrich, St. Louis, MO) at 37° until the solution became cloudy and the mesenchyme was dissociated. A single-cell suspension was obtained by collecting the supernatant and washing with Hank's balanced salt solution before cell sorting using a BD influx instrument (BD Biosciences, San Jose, CA). For RNA isolation, YFP+ cells were lysed and total RNA was isolated by column purification (Agilent Technologies). Messenger RNA (mRNA) was isolated using Poly(A) mRNA isolation magnetic beads and an mRNA sequencing library prepared using the NEBNext RNA library prep kit (New England BioLabs, Inc, Ipswich, MA). RNA sequencing was performed on an Illumina HiSeq instrument.

RNA Isolation and Library Formation From Crypt Cells

To isolate RNA from intestinal crypts after diphtheria toxin injection, *Foxl1–hDTR* and control mice were injected with diphtheria toxin at 20 ng/g body weight on day 0 and euthanized on day 3. Dissected intestines were washed in PBS to remove the luminal content, incubated in 5 mmol/L

Table 1. Primer Sequences

Cdh1 Fw	GGCTTCAGTTCCGAGGTCTA
Chd2 Rv	CTCTGGGTTGGATTCAGAGG
Vim Fw	GATCAGCTCACCAACGACAA
Vim Rv	TCCGGTACTCGTTTGACTCC
HBEGF Fw	ACTTTATCCTCCAAGCCACAAG
HBEGF Rv	CCCAGATACCATCGGACATACT

Fw, forward; Rv, reverse.

EDTA in PBS for 10 minutes, and scraped with a coverslip gently to remove villus cells. The remaining tissue was cut into 5-mm pieces and incubated in 5 mmol/L EDTA for 20 minutes with vigorous pipetting every 2–3 minutes. The tissue was washed and pipetted vigorously, and floating crypts were collected. Crypt RNA was isolated using TRIzol reagent (Life Technologies, Carlsbad, CA) and subjected to Poly-A selection using magnetic isolation (New England BioLabs, Inc). Libraries were prepared with the RNA Library Prep Kit (New England BioLabs, Inc) and sequenced using an Illumina HiSeq instrument.

Histology

For H&E staining, paraffin tissue sections were rehydrated, incubated in hematoxylin for 2.5 minutes, rinsed in water, dipped quickly in 0.5% acid alcohol, and washed in water. Tissues then were immersed in 0.2% $NaHCO_3$, rinsed in water, dipped in eosin for 15 seconds, and briefly rinsed in water before dehydration and mounting.

Immunofluorescence and Immunohistochemistry

At time of death, mouse intestines were rinsed in PBS and fixed with 4% paraformaldehyde overnight, rinsed in PBS, and either dehydrated for paraffin embedding or immersed in 30% sucrose for 4 hours at 4°C, embedded in optimum cutting temperature compound (OCT), and frozen for cryosectioning. Antigen retrieval was achieved using citrate buffer, pH 6.0, with a pressure cooker (PickCell Laboratories, Agoura Hills, CA). Foxl1 staining required the use of cryosections, antigen retrieval, and amplification of signal using tyramide (TSA systems; PerkinElmer, Waltham, MA). Antibodies used were as follows: Ki67 (1:500; BD Pharmingen, Franklin Lakes, NJ), lysozyme (1:1000; Dako, Carpinteria, CA), Sox9 (1:300; Millipore, Temecula, CA), mucin 2, HBEGF (1:50; Santa Cruz Biotechnology, Dallas, TX), guinea pig Foxl1 (1:1500), goat green fluorescence protein (1:200; Abcam, Cambridge, MA), mouse E-cadherin (1:250; BD Transduction, Franklin Lakes, NJ), mouse β-catenin (1:200; BD Transduction), rabbit EpCAM (1:100; Abcam), rabbit α-smooth muscle actin (1:100; Abcam), and rabbit myosin heavy chain 11 (Myh11) (1:100; Abcam). Cy2-, Cy3-, and Cy5-conjugated donkey secondary antibodies were purchased from Jackson ImmunoResearch Laboratories, Inc. For immunohistochemistry, horseradish-peroxidase–conjugated secondary antibodies were incubated at room temperature for 2 hours. The Vectastain ABC kit (Vector Laboratories, Burlingame, CA) then was used to detect the signal, and the slides were washed with PBS. For signal development, the 3,3′-diaminobenzidine tetra hydrochloride substrate was used.

In Situ Hybridization

Olfm4 RNA in situ hybridization was performed as previously described using ornithine carbamyl transferase–embedded frozen tissues.[7,19] For other in situ hybridization experiments, double digoxigenin-labeled locked nucleic acid probes were designed (Exiqon, Vedbaek, Denmark). Paraffin sections were rehydrated, fixed, and pretreated as described by Silahtaroglu[20] with the following modifications: in addition to acetylation, slides

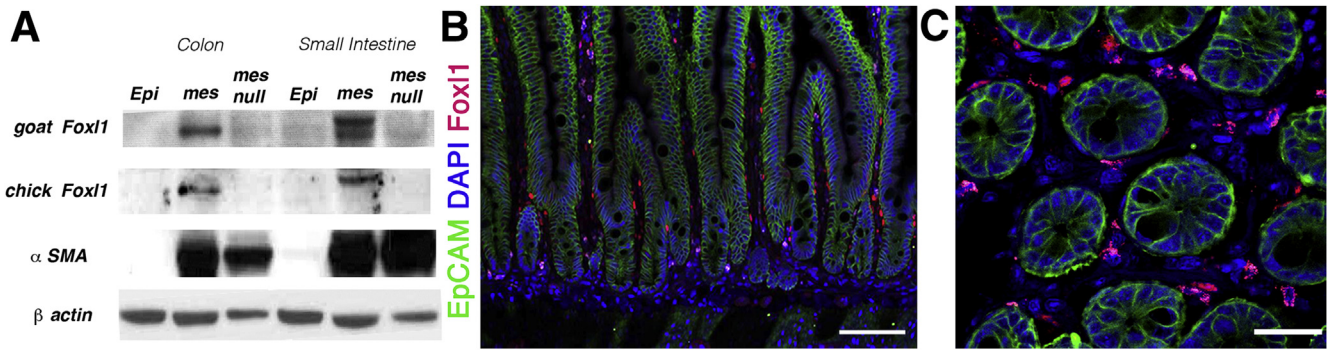

Figure 1. Antibodies to the mouse Foxl1 protein are specific, and Foxl1 is expressed in a small subset of subepithelial fibroblasts in the intestine. (*A*) Immunoblot analysis for the Foxl1 protein in epithelial and mesenchymal fractions of mouse small intestine (jejunum) and colon, as indicated. Two different affinity-purified anti-Foxl1 antibodies were used. Note the absence of the Foxl1 protein band in mesenchymal fractions from Foxl1 null mice. Immunoblot analysis of α-smooth muscle actin (αSMA) confirms separation of epithelium and mesenchyme. mes, mesenchyme. (*B*) Immunostaining showing expression of Foxl1 (red) in the adult small intestine in a subset of mesenchymal cells located in close apposition to the epithelium (outlined with immunostaining for EpCAM, green). Nuclei are labeled with 4′,6-diamidino-2-phenylindole (DAPI) (blue). *Scale bar*: 50 μm. (*C*) Cross-section of crypt region showing the localization of Foxl1+ cells (red) in pericryptal mesenchymal cells. Nuclei are labeled with DAPI (blue). *Scale bar*: 25 μm.

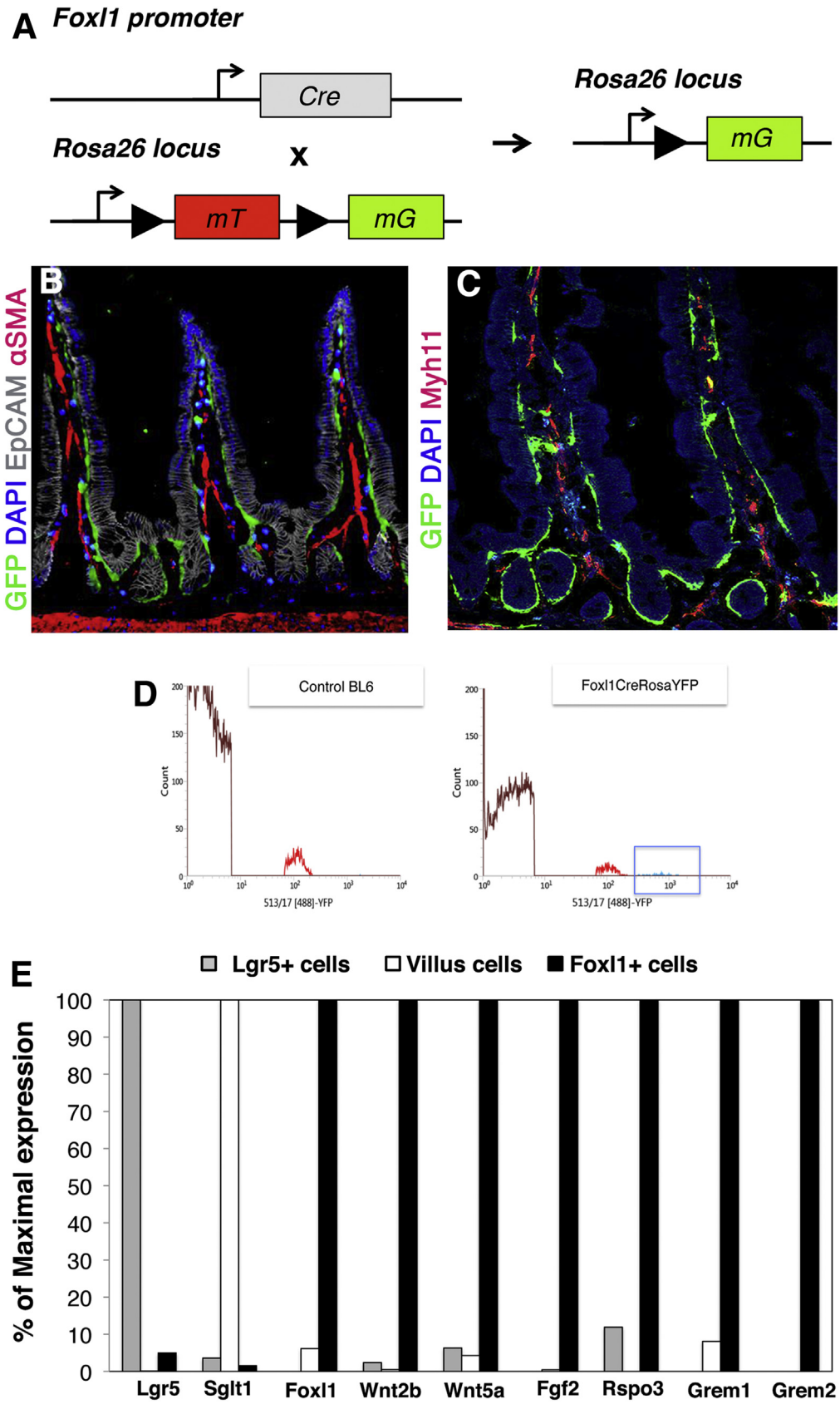

Figure 2. Foxl1+ cells have long processes and express potential niche-supporting factors. (*A*) Schema of Foxl1–Cre; Rosa–membrane-targeted dimer tomato protein membrane-targeted green fluorescent protein mouse used to drive expression of a membrane-bound green fluorescence protein (GFP) in Foxl1-Cre–positive cells. (*B*) Foxl1–Cre–driven expression of membrane-bound GFP is restricted to pericryptal mesenchymal cells, which elaborate long extensions into the villus tips and surrounding intestinal crypts. Immunofluorescence staining for GFP (green) and α-smooth muscle actin (αSMA) (red) shows very limited overlap between the 2 markers, indicating that Foxl1+ cells represent a unique cell population. αSMA expression is present in the core of the lamina propria, whereas GFP expression is located at the pericryptal sheath. (*C*) Immunofluorescence staining for Foxl1–Cre–driven GFP (green) and Myh11 (red) indicates very limited overlap between the 2 markers. (*D*) A histogram of fluorescence-activated cell sorting of intestinal mesenchymal cells isolated from C57BL6 control and Foxl1–Cre;Rosa–YFP mice using YFP fluorescence. The x-axis shows YFP fluorescence intensity, and the gate indicated in the Foxl1–Cre;Rosa–YFP plot shows the sorted cells from which RNA was isolated for RNA sequence analysis. Note the absence of high-intensity YFP+ cells in the control histogram. (*E*) Relative mRNA levels of various markers and key signaling molecules in sorted Lgr5+-epithelial stem cells, differentiated villus epithelial cells, and sorted Foxl1+ cells.

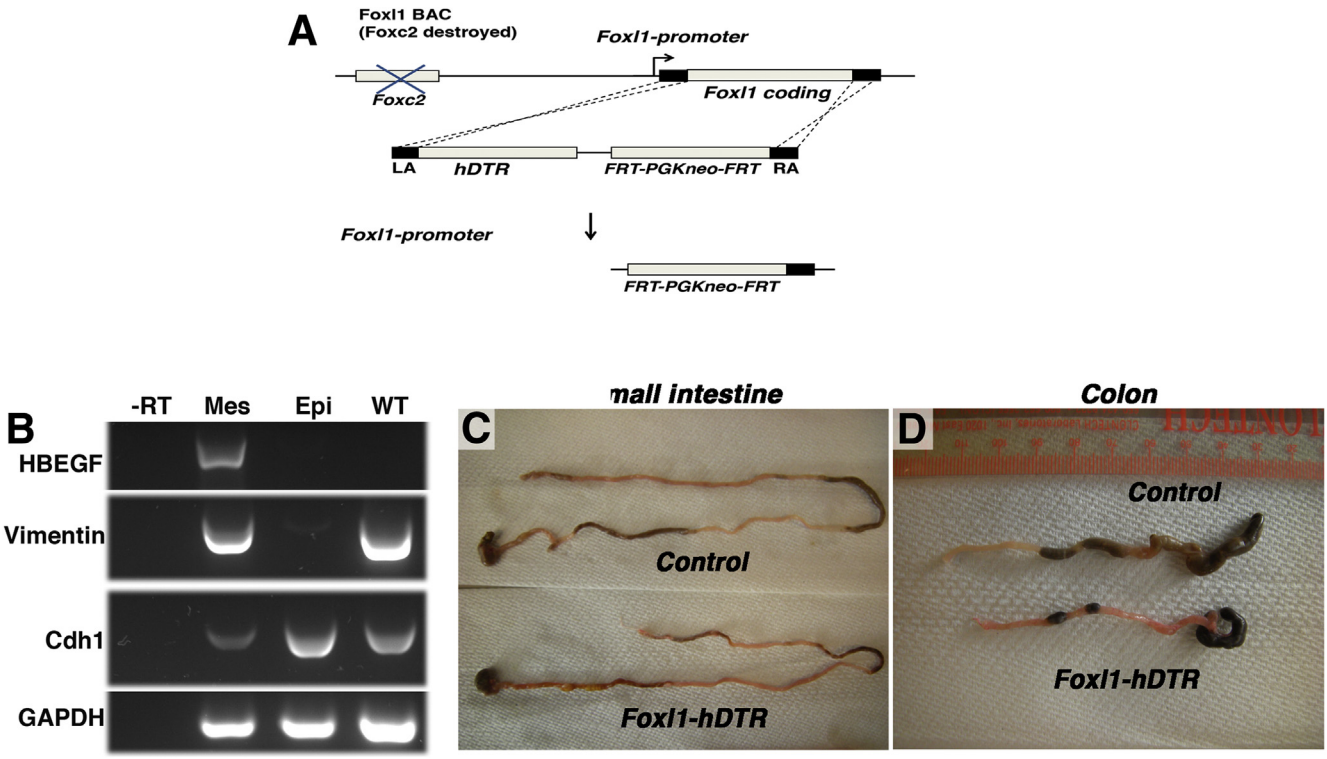

Figure 3. Ablation of Foxl1+ mesenchymal cells in diphtheria toxin–treated Foxl1–hDTR mice results in shortening of the gut tube. (*A*) Schema for the generation of Foxl1–hDTR mice using BAC recombineering. The coding sequence of exon 1 of *Foxl1* was targeted by the sequence of the hDTR after destruction of the upstream *FoxC2* coding sequence. FRT, flippase recognition target; LA, left homology arm; RA, right homology arm. (*B*) Expression of the human diphtheria toxin receptor (the *HBEGF* gene) is confined to the mesenchyme in Foxl1–hDTR mice. Mesenchyme and epithelium of the colon from Foxl1–hDTR mice were separated and cDNA was prepared. Reverse-transcription PCR analysis was performed to detect mesenchymal vimentin, epithelial E-cadherin, and ubiquitous glyceraldehyde-3-phosphate dehydrogenase (GAPDH) transcripts. Note that the HBEGF/hDTR mRNA is present exclusively in the mesenchyme. -RT, without reverse transcriptase; Mes, mesenchyme; Epi, epithelium; WT, whole colon from control nontransgenic mice. (*C* and *D*) Representative images of small intestine and colon from DT-treated Foxl1–hDTR and control mice. Note the shortening of the gut tube in the DT-treated Foxl1–hDTR mice.

were pretreated with 10 ng/mg proteinase K for 10 minutes at 37°, and 80 nmol/L of probe mixture was used for hybridization. 4′,6-Diamidino-2-phenylindole was used to mark the nuclei (Vector Laboratories).

Western Blot

Small and large intestines were dissected from C57Bl/6 control and Foxl1-null[7] mice. Isolated tissues were washed with PBS and scraped with a coverslip to remove the villus epithelium. Intestinal epithelial cells were separated from mesenchymal cells as described in fluorescent-activated cell sorting and RNA isolation. Tissues then were subjected to multiple rounds of sonication to lyse the cells in buffer containing 50 mmol/L Tris (pH 8.0), 150 mmol/L NaCl, 1 mmol/L EDTA, 1% Triton X-100, 0.5% deoxycholic acid, and 1% sodium dodecyl sulfate, supplemented with protease inhibitor cocktail (Roche, Indianapolis, IN) and phosphatase inhibitor cocktails 1 and 2 (Sigma-Aldrich). Cell lysates were separated by sodium dodecyl sulfate–polyacrylamide gel electrophoresis and transferred to polyvinylidene difluoride membranes with the iBlot system (Life Technologies). Membranes were blocked in blocking buffer consisting of 5% milk and 0.1% Tween-20 in PBS for 2 hours and incubated with antibodies at 4° overnight in blocking buffer. Antibodies used were as follows: chicken Foxl1 (1:500), goat Foxl1 (1:500), mouse α-smooth muscle actin (1:10,000; Sigma), mouse E-cadherin (1:5000; BD Transduction), rabbit β-actin (1:10,000; Cell Signaling, Danvers, MA). Membranes then were washed and incubated with horseradish-peroxidase–conjugated goat-anti-rabbit IgG.

Fractional Separation of Mesenchyme and Reverse-Transcription PCR

Intestines from adult *Foxm1–hDTR* mice were cut open and washed in PBS. Intestinal epithelial cells were separated from mesenchymal cells as described in fluorescent-activated cell sorting and RNA isolation. The crypt epithelium was scraped off and collected. To ensure isolation of pure epithelium, epithelial cells were incubated in 0.05% trypsin to obtain single cells, followed by incubation with an Alexa-488 mouse EpCAM (1:250; Biolegend, San Diego, CA)

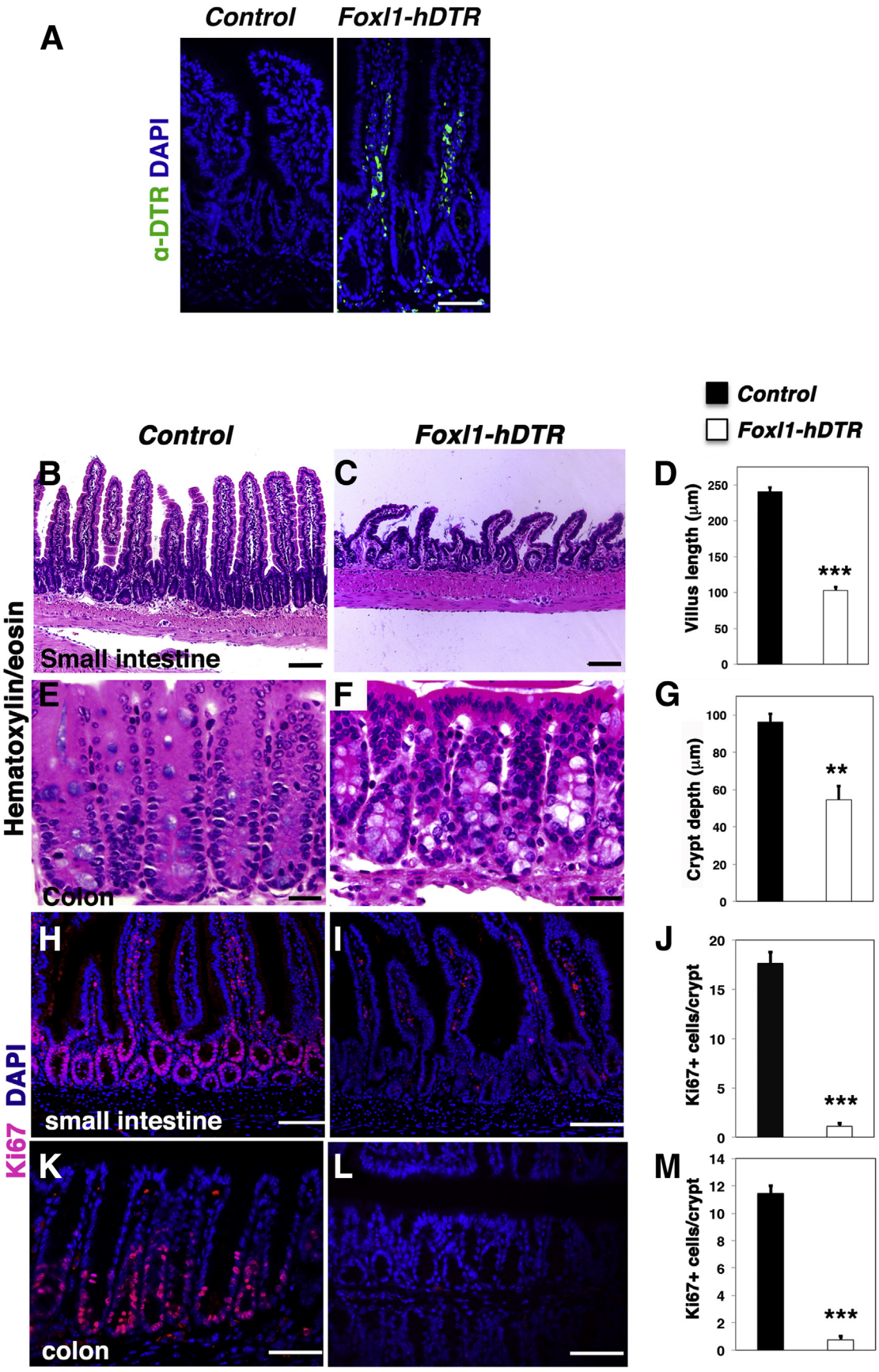
A
Control
Foxl1-hDTR
α-DTR DAPI
Control
Foxl1-hDTR
Hematoxylin/eosin
B
C
Small intestine
E
F
Colon
Ki67 DAPI
H
I
small intestine
K
L
colon
Control
Foxl1-hDTR
D
Villus length (μm)
250
200
150
100
50
0
***
G
Crypt depth (μm)
100
80
60
40
20
0
**
J
Ki67+ cells/crypt
20
15
10
5
0
***
M
Ki67+ cells/crypt
14
12
10
8
6
4
2
0
***

antibody, and sorted in a BD Influx instrument (BD Biosciences). The remaining mesenchymal tissue was washed to remove any epithelial contamination. From the epithelial and mesenchymal fractions, RNA was isolated and complementary DNA (cDNA) was synthesized. For mesenchymal and epithelial-specific markers as well as *hDTR*, reverse-transcription PCR was performed using GoTaq (Promega, Madison, WI). The primers used in this experiment are listed in Table 1.

Results

Foxl1 Is Expressed in a Subset of Mesenchymal Cells

We hypothesized that mesenchymal cells in close apposition to the crypt epithelium constitute the intestinal stem cell niche in vivo. We and others[21–23] have shown that the winged-helix transcription factor Foxl1 (previously known as *Fkh6*) is expressed specifically in the gastrointestinal mesenchyme during fetal development and in adulthood. We developed new Foxl1-specific antibodies to map the location of this cell type in the mammalian gut more precisely. We established the specificity of these affinity-purified antibodies through immunoblot analysis of *Foxl1*-null gut tissue (Figure 1*A*). Foxl1 protein was confined to the nuclei of a subset of subepithelial cells that are tightly apposed to the epithelium of small intestinal crypts, with some cells extending into the villus tip (Figure 1*B* and *C*).

Foxl1+ Cells Are Distinct From Myofibroblasts and Express Potential Niche-Supporting Factors

To better define the relationship of Foxl1-expressing cells to established mesenchymal cell types, we used Foxl1–Cre;Rosa–mT/mG mice, in which Foxl1 promoter-dependent Cre activity results in the expression of a plasma membrane-bound green fluorescence protein (Figure 2*A*, scheme) (see Materials and Methods section for details), which allowed us to visualize the Foxl1-expressing cells in their full extension. As shown in Figure 2*B*, Foxl1+ cells elaborate long processes that span the width of multiple epithelial cells, suggesting that Foxl1+ cells are placed in an optimal position for short-range signaling to the epithelium. Dual-label immunofluorescence staining clearly showed that the Foxl1+ cell is distinct from mesenchymal cells expressing the smooth muscle markers α-smooth muscle actin (Figure 2*B*) and Myh11 (Figure 2*C*).

Next, we used fluorescence-activated cell sorting to enrich for mesenchymal cells expressing Foxl1–Cre (Figure 2*D*). When we compared the mRNA levels of key genes between Foxl1+ mesenchymal cells and either Lgr5+ epithelial stem cells or differentiated intestinal villus cells (data from[24]), we found, as expected, that the Foxl1+ fraction did not express Lgr5 or the sodium/glucose cotransporter Sglt1, markers of epithelial stem and differentiated villus cells, respectively (Figure 2*E*). However, the mesenchymally expressed Wnt genes Wnt2b and Wnt5a were highly enriched in Foxl1+ pericryptal fibroblasts, suggesting that it is these cells that provide critical Wnt signals to the intestinal stem cell compartment. In addition, Foxl1+ cells express high levels of R-spondin 3, an activator of Went signaling,[25] fibroblast growth factor 2, and gremlin 1 and 2, antagonists of the bone morphogenetic protein pathway that are expressed in intestinal reticular stem cells.[26]

Ablating Foxl1+ Cells Leads to Disrupted Epithelium

Because of this unique expression pattern, the elaboration of key signaling molecules, and because ablation of the *Foxl1* gene itself causes altered Wnt signaling in stomach and intestine,[27] we surmised that Foxl1-expressing mesenchymal cells might constitute the intestinal stem cell niche. To test this hypothesis, we derived mice transgenic for a bacterial artificial chromosome comprising 170 kb of the *Foxl1* locus in which the Foxl1 coding region was replaced by the hDTR cDNA (Foxl1–hDTR mice) (Figure 3*A*). Although mice are normally resistant to diphtheria toxin, expression of the hDTR in Foxl1-expressing (Foxl1+) mesenchymal cells renders these cells diphtheria toxin–sensitive, leading to cell-specific apoptosis after toxin administration. As expected, expression of the human diphtheria toxin receptor was confined to the subepithelial mesenchyme (Figures 3*B* and 4*A*).

Strikingly, after 3 days of exposure to diphtheria toxin, the length of the small and large intestines was reduced in Foxl1–hDTR mice (Figure 3*C* and *D*).

Figure 4. (***See previous page***). **Intestinal epithelial architecture and proliferation are dependent on Foxl1+ mesenchymal cells.** (*A*) Representative immunofluorescence images of human diphtheria toxin receptor (green) staining in the jejunum of control and Foxl1–hDTR mice, counterstained with 4′,6-diamidino-2-phenylindole (DAPI) to label nuclei (blue). (*B* and *C*) Intestinal morphology of the jejunum of (*B*) DT-treated control mice or (*C*) Foxl1–hDTR mice as assessed by H&E staining. Note the reduced number and length of intestinal villi in Foxl1–hDTR mice. (*D*) Quantification of small intestinal villus length (n = 4; in each animal > 20 villi were measured; ***$P < .001$). (*E* and *F*) Intestinal morphology of the proximal colon from (*E*) DT-treated control and (*F*) Foxl1–hDTR mice. Note the decreased depths of the colonic crypts and the irregular localization of epithelial nuclei in Foxl1–hDTR mice. (*G*) Quantification of colonic crypt depth (n = 4; in each animal > 20 crypts were measured; **$P < .005$). (*H* and *I*) Representative immunofluorescence images of the proliferation marker Ki67 (red) counterstained with DAPI to label nuclei (blue) in the jejunum of (*H*) control and (*I*) Foxl1–hDTR mice after toxin injection. (*J*) Quantification of the number of proliferating cells per crypt unit in jejunum of DT-treated control and Foxl1–hDTR mice (n = 20 crypts each). ***$P < .001$. (*K* and *L*) Ki67 labeling (red) overlaid with DAPI for nuclei (blue) in the colon of (*K*) DT-treated control and (*L*) Foxl1–hDTR mice. The number of Ki67-positive cells is reduced dramatically in Foxl1–hDTR mice. *Scale bars*: 50 μm. (*M*) Quantification of the number of proliferating cells per crypt unit in the proximal colon of DT-treated control and Foxl1–hDTR mice (n = 20 crypts each). ***$P < .001$.

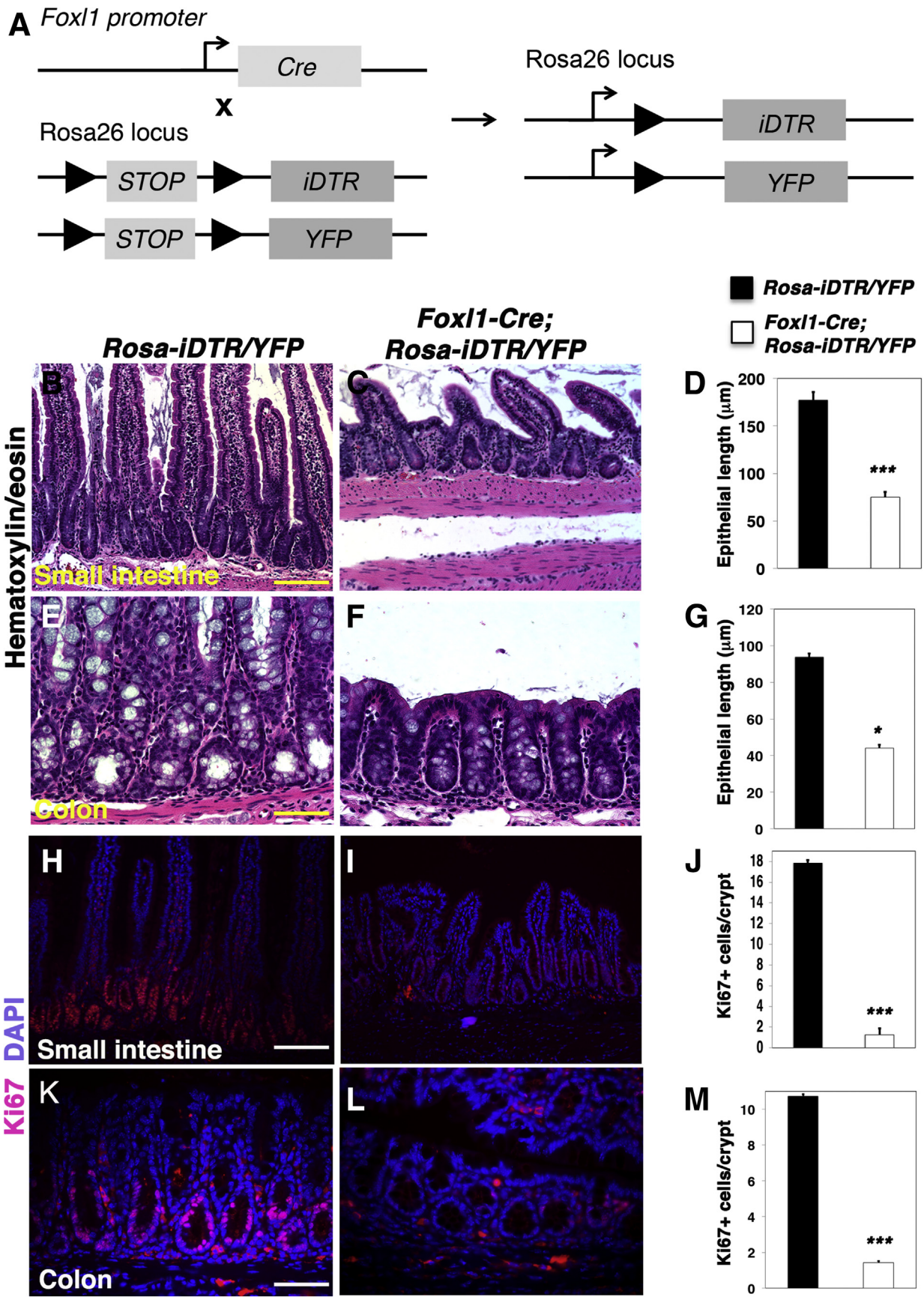
A
Foxl1 promoter
Cre
x
Rosa26 locus
STOP
iDTR
STOP
YFP
Rosa26 locus
iDTR
YFP
Rosa-iDTR/YFP
Foxl1-Cre; Rosa-iDTR/YFP
Rosa-iDTR/YFP
Foxl1-Cre; Rosa-iDTR/YFP
Hematoxylin/eosin
B
C
Small intestine
E
F
Colon
D
Epithelial length (μm)
200
150
100
50
0
***
G
Epithelial length (μm)
120
100
80
60
40
20
0
*
DAPI
H
I
Small intestine
J
Ki67+ cells/crypt
18
16
14
12
10
8
6
4
2
0
***
Ki67
K
L
Colon
M
Ki67+ cells/crypt
10
8
6
4
2
0
***

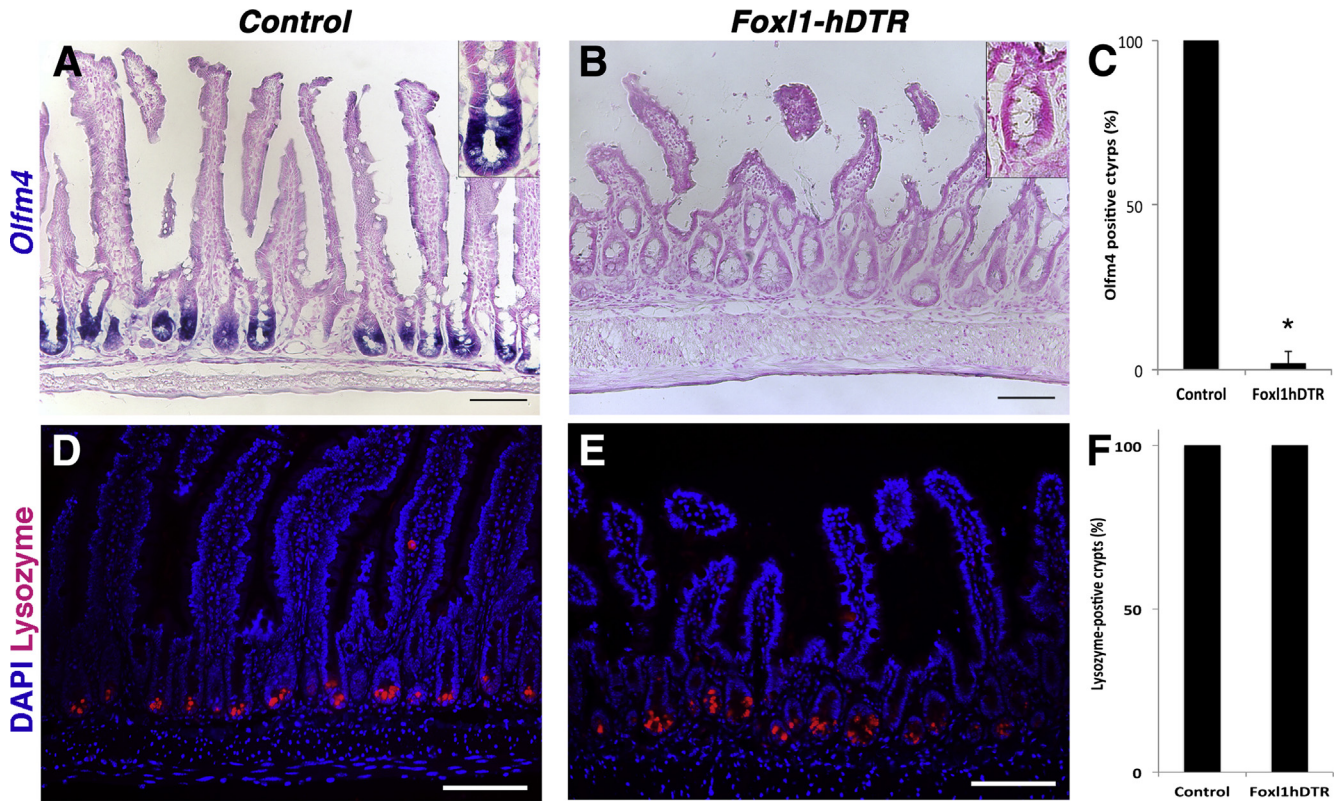

Figure 6. Foxl1+ mesenchymal cells are required for intestinal stem cell marker expression independent of Paneth cells. (*A* and *B*) Expression of the intestinal stem cell marker Olfm4 is reduced in (*B*) DT-treated Foxl1–hDTR mice compared with (*A*) nontransgenic controls as determined by in situ hybridization. Insets show crypts at high magnification. (*C*) Quantification of the percentage of small intestinal crypts that are positive for *Olfm4* mRNA (>200 crypts were counted for both DT-treated control and *Foxl1*–hDTR mice). *$P < .01$. (*D* and *E*) Expression of lysozyme (red), a Paneth cell marker, is not affected by ablating Foxl1+ cells. *Scale bar*: 50 μm. (*F*) Quantification of lysozyme-positive cells per crypt unit (n = 3 per genotype; >20 crypts were evaluated per animal). DAPI, 4′,6-diamidino-2-phenylindole.

Foxl1–hDTR mice showed dramatic changes to the architecture of the small and large intestine (Figure 4*B*, *C*, *E*, and *F*). The length of the villi was reduced dramatically in the jejunum (Figure 4*D*), and epithelial architecture was abnormal in colonic crypts, which showed reduced depth (Figure 4*G*). To test our hypothesis that Foxl1+ mesenchymal cells constitute an essential part of the intestinal stem and progenitor cell niche, we next analyzed gut tissue for epithelial proliferation. Immunofluorescence labeling for the proliferation marker Ki67 showed that the deletion of Foxl1+ mesenchymal cells resulted in a dramatic and highly significant reduction of epithelial cell proliferation in the jejunum (Figure 4*H–J*) and colon (Figure 4*K–M*).

Figure 5. (***See previous page***). **Targeted ablation of Foxl1+ mesenchymal cells using the iDTR model causes loss of epithelial proliferation.** (*A*) Schema for the generation of Foxl1–iDTR mice. Foxl1–Cre mice were crossed to mice carrying a loxP-stop-loxP simian diphtheria toxin–receptor construct in the Rosa26 locus ($Rosa^{iDTR}$ mice). (*B* and *C*) Small intestinal (jejunum) morphology was assessed by H&E staining of (*B*) DT-treated control and (*C*) Foxl1–iDTR mice. Note the reduced number and length of intestinal villi. (*D*) Quantification of small intestinal villus length (n = 4; in each animal > 20 villi were evaluated per mouse; ***$P < .001$). (*E* and *F*) Colonic morphology of (*E*) DT-treated control and (*F*) Foxl1–iDTR mice. Decreased depths of the colonic crypts is apparent in Foxl1–iDTR mice. (*G*) Quantification of colonic crypt depth (n = 4; in each animal >20 crypts were evaluated per mouse; *$P < .05$). (*H* and *I*) Representative immunofluorescence images of small intestinal (jejunum) sections stained for the proliferation marker Ki67 (red) and counterstained with 4′,6-diamidino-2-phenylindole (DAPI) to label nuclei (blue) of (*H*) control and (*I*) Foxl1–iDTR mice. The number of Ki67-positive epithelial cells is reduced dramatically in Foxl1–iDTR mice. (*J*) Quantification of the number of proliferating cells per crypt unit in the jejunum of DT-treated control and Foxl1–iDTR mice (n = 20 crypts each). ***$P < .001$. (*K* and *L*) Ki67 labeling (red) overlaid with DAPI to mark nuclei (blue) in the colon of (*K*) DT-treated control and (*L*) Foxl1–iDTR mice. The number of Ki67-positive cells is reduced dramatically in Foxl1–iDTR mice. (*M*) Quantification of the number of proliferating cells per crypt unit in the colon of DT-treated control and Foxl1–iDTR mice (n = 20 crypts each). ***$P < .001$. *Scale bars*: 100 μm in the small intestine, 50 μm in the colon.

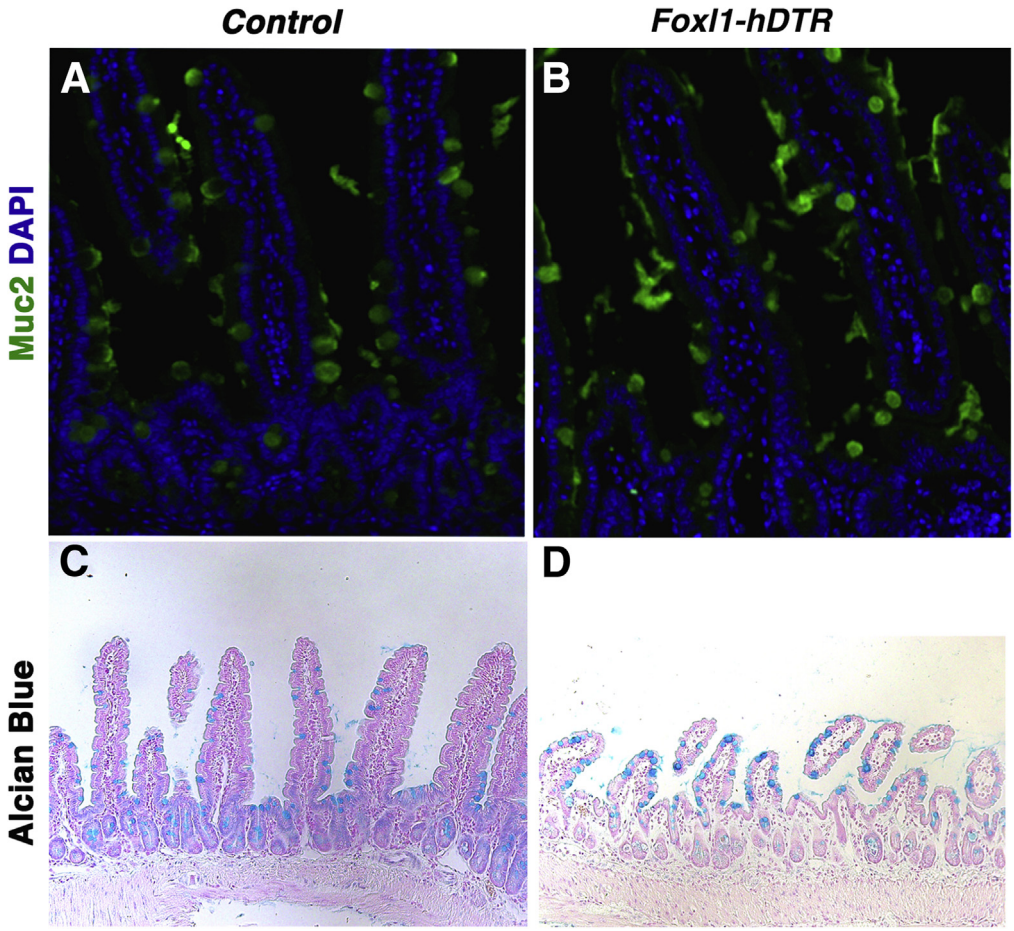

Figure 7. The frequency of mucin-secreting goblet cells is unaffected by ablation of Foxl1+ cells. (*A* and *B*) Detection of goblet cells by immunostaining for Muc2 (mucin 2; green) and (*C* and *D*) Alcian Blue histochemistry (blue) indicates that the frequency of goblet cells in (*B* and *D*) DT-treated *Foxl1–hDTR* mice is not different from that present in (*A* and *C*) control mice. DAPI, 4′,6-diamidino-2-phenylindole.

Ablating Foxl1+ Cells by a Separate Model Leads to Similar Epithelial Disruption

Next, we used an independent paradigm (Figure 5*A*) (Foxl1–Cre;Rosa–iDTR mice; see the Materials and Methods section for experimental details) in which expression of the simian DTR is activated in Foxl1-positive cells through Cre-mediated deletion of a stop cassette, again making cells susceptible to diphtheria toxin.[28,29] Remarkably similar results were obtained with this second cell-ablation model, in which again villus length and crypt depth were reduced significantly in the jejunum and colon, respectively (Figure 5*B–G*). Likewise, epithelial proliferation was reduced dramatically in diphtheria toxin–treated Foxl1–Cre, Rosa–iDTR mice (Figure 5*H–M*). Taken together, these results show that Foxl1-expressing mesenchymal cells are required for maintaining proliferation of the intestinal epithelium, both in stem cells and in the derived transit-amplifying cell population.

Stem Cells but Not Paneth Cells Are Affected by Ablating Foxl1+ Cells

In addition to loss of proliferation, expression of the stem cell marker *Olfm4* was reduced dramatically in mice with ablation of Foxl1+ subepithelial mesenchymal cells (Figure 6*A–C*). However, the long-lived lysozyme-expressing Paneth cells were retained in the small intestinal epithelium of diphtheria toxin–treated Foxl1–hDTR mice, indicating that loss of epithelial proliferation was not secondary to loss of Paneth cells (Figure 6*D–F*).

Moreover, cell-lineage allocation among the differentiated lineages was not affected globally in the 3 days from toxin administration to analysis, as evidenced by the presence of mucin 2 and Alcian Blue–positive goblet cells (Figure 7*A–D*).

Ablating Foxl1+ Cells Leads to Reduced Wnt Signaling

Proliferation of the intestinal epithelium is driven by Wnt signaling,[9,10,30] and we hypothesized that Foxl1-expressing subepithelial cells serve as an essential source of these signals. To determine if Wnt signaling is affected by loss of Foxl1+ cells, we evaluated nuclear β-catenin staining. As shown in Figure 8*A* and *B*, nuclear β-catenin expression was greatly reduced in the crypts of Foxl1–hDTR mice after diphtheria-toxin administration, which was indicative of loss of canonical Wnt signaling activity. Next, we investigated the expression of the Wnt target gene *Sox9* in Foxl1–hDTR mice after diphtheria toxin administration. Sox9 protein normally is present in the entire crypt, including

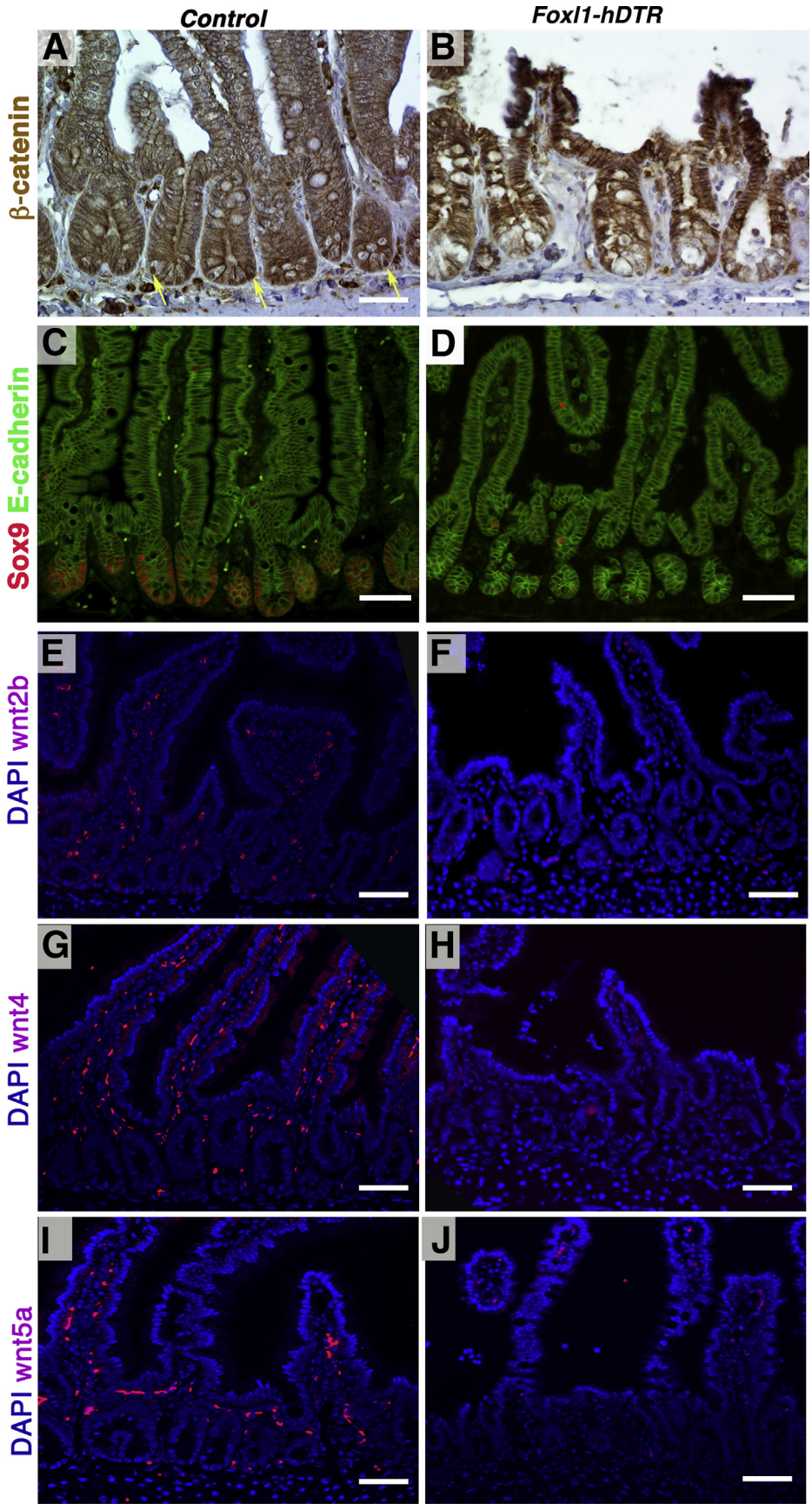

Figure 8. Foxl1+ mesenchymal cells provide essential Wnt ligands to the intestinal stem cell compartment. (*A* and *B*) Activation of the Wnt pathway in epithelial cells of the jejunum was analyzed by immunohistochemistry for ß-catenin. Reduced nuclear ß-catenin localization is apparent in (*B*) toxin-treated *Foxl–hDTR* mice compared with (*A*) toxin-treated controls. *Yellow arrows* point to nuclei positive for ß-catenin. *Scale bars*: 25 μm. (*C* and *D*) Immunofluorescence staining of the Wnt target Sox9 (red) shows decreased expression in the jejunum of (*D*) DT-treated *Foxl1–hDTR* mice compared with (*C*) nontransgenic controls. The epithelium is delineated with E-cadherin immunostaining (green). *Scale bars*: 50 μm. (*E* and *F*) Mesenchymal Wnt2b mRNA was detected by in situ hybridization (red) and nuclei were counterstained with 4′,6-diamidino-2-phenylindole (DAPI) (blue) Wnt2b mRNA is reduced dramatically in the mesenchyme of (*F*) DT-treated *Foxl1–hDTR* mice compared with (*E*) controls. *Scale bars*: 50 μm. (*G* and *H*) Mesenchymal Wnt4 and (*I* and *J*) Wnt5a mRNAs were detected by in situ hybridization (red) and nuclei were counterstained with DAPI (blue). Wnt4 and Wnt5a mRNA levels were reduced dramatically in the mesenchyme of (*H* and *J*) DT-treated *Foxl1–hDTR* mice compared with (*G* and *I*) controls.

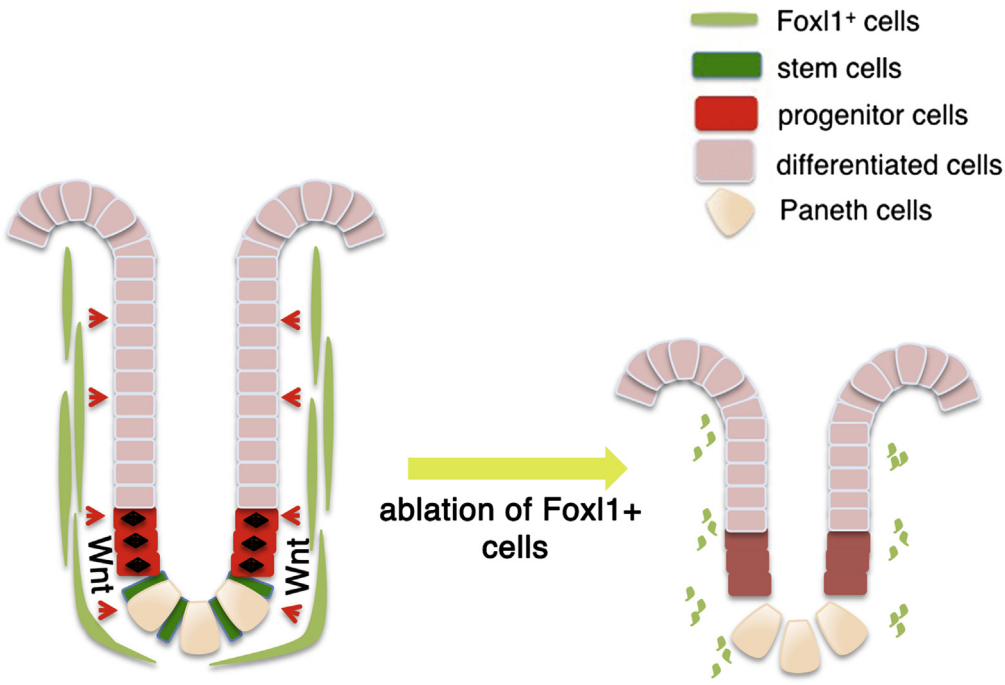

Figure 9. Proposed model of Foxl1-positive subepithelial mesenchymal cells as the intestinal stem cell niche, providing essential Wnt signals, and possibly other signaling molecules, to the epithelium.

intestinal stem cells and Paneth cells.[31] After diphtheria toxin treatment, we noted a striking decrease in the number of Sox9-expressing cells in Foxl1–hDTR crypts as compared with controls (Figure 8*C* and *D*), again supporting reduced Wnt signaling activity.

Both canonical and noncanonical Wnt factors are produced by the intestinal mesenchyme.[15,19] Farin et al[15] established Wnt2b as a mesenchymal Wnt protein that is sufficient to support intestinal organoid growth in culture. Strikingly, Wnt2b, Wnt4, and Wnt5a signals that are normally detected in the subepithelial mesenchyme were decreased dramatically in Foxl1–hDTR mice after diphtheria toxin administration (Figure 8*E–J*). These data suggest that production of Wnt2b, Wnt4, and Wnt5a by Foxl1-expressing mesenchymal cells, which are located in close proximity to the basement membrane of the epithelial crypt, is part of the signal required to maintain the intestinal stem cell niche.

Discussion

Wnt signaling is required for the maintenance of the adult intestine; however, the cellular source of this ligand has not been defined satisfactorily. Although Sato et al[11] deduced that Paneth cells are this source because they express and secrete Wnt ligands, and because co-culture of Paneth cells and Lgr5+ cells allows the formation of intestinal organoids, several lines of evidence challenged the view of the Paneth cell as an absolutely required in vivo source of signals required to maintain the intestinal stem cell. For example, loss of Paneth cells[12,13] or loss of the essential Wnt-processing protein Porcupine (*Porcn*) in Paneth cells[32,33] has no effect on intestinal stem cell maintenance.

An alternative source for the signals required for stem cell maintenance is the intestinal mesenchyme. Recently, however, San Roman et al[33] showed that *Porcn*, and therefore the Wnt signal, do not originate solely from Myh11-expressing intestinal smooth muscle cells and myofibroblasts or, independently, from villin-expressing epithelial cells. Kabiri et al[33] ablated *Porcn* expression from the entire intestinal epithelium using villin-Cre and showed normal intestinal morphogenesis. Together, these studies suggested that either redundant Wnt signaling from both epithelial and mesenchymal compartments or a rare Wnt-producing cell type in one of these compartments that had not been targeted with the existing Cre lines is responsible for crypt maintenance.

We show here that Foxl1+ mesenchymal cells exist independently of the Myh11-expressing subepithelial myofibroblasts targeted by San Roman et al[33] (Figure 1). Thus, the rare Foxl1+ cells that reside in the intestinal mesenchyme, in close apposition to the intestinal crypt, are outstanding candidates to be the minor Wnt-producing cell type in the intestine postulated by San Roman et al.[33]

These Foxl1+ cells are located directly adjacent to the epithelium and extend long processes that span the length of multiple epithelial cells. They express Wnt2b, Wnt4, and Wnt5a, and the loss of these Foxl1+ cells results in decreased β-catenin nuclear localization and proliferation within the intestinal epithelium, reduced villi length, diminished crypts depths, and an overall shortening of the intestine. Therefore, Foxl1+ cells are required for intestinal stem cell maintenance and are not functionally redundant with Wnt-expressing Paneth cells.

We considered whether the diphtheria-toxin–mediated killing of Foxl1+ cells might have indirect effects on the

intestinal stem cell niche not mediated by controlling physiological signaling components such as the Wnt proteins described earlier. For instance, one might envisage a bystander effect in which debris from dying Foxl1+ cells is taken up by intestinal stem cells, leading to their death. We consider this scenario exceedingly unlikely, considering that diphtheria toxin–mediated ablation of Paneth cells, which after all are abutting Lgr5+ stem cells directly, is without an effect on crypt health.[14]

Of note, mice deficient for the winged helix transcription factor Foxl1, although showing abnormal gastrointestinal development,[23] are viable and maintain functioning crypts. In fact, the role of Foxl1 and its direct targets is in limiting Wnt signaling to the epithelial compartment.[23] Of course, it is not surprising that the genetic ablation of one gene within a cell does not have the same consequences as ablating that cell type entirely because each transcription factor controls only part of the transcriptional program within the cell.

Although the cellular identity of the intestinal stem cell niche has been controversial until this point, by using 2 novel, independent, cell-ablation models, we show that Foxl1+ subepithelial mesenchymal cells are the source of essential Wnt signals and thus constitute the intestinal stem and progenitor cell niche (model in Figure 9). Positive identification of the cells that provide the intestinal stem cell niche might aid in the future development of regenerative strategies for intestinal disorders.

References

1. Barker N, van Es JH, Kuipers J, et al. Identification of stem cells in small intestine and colon by marker gene Lgr5. Nature 2007;449:1003–1007.
2. Sangiorgi E, Capecchi MR. Bmi1 is expressed in vivo in intestinal stem cells. Nat Genet 2008;40:915–920.
3. Takeda N, Jain R, LeBoeuf MR, et al. Interconversion between intestinal stem cell populations in distinct niches. Science 2011;334:1420–1424.
4. von Furstenberg RJ, Gulati AS, Baxi A, et al. Sorting mouse jejunal epithelial cells with CD24 yields a population with characteristics of intestinal stem cells. Am J Physiol Gastrointest Liver Physiol 2011;300:G409–G417.
5. Powell AE, Wang Y, Li Y, et al. The pan-ErbB negative regulator Lrig1 is an intestinal stem cell marker that functions as a tumor suppressor. Cell 2012;149:146–158.
6. Wright NA, Irwin M. The kinetics of villus cell populations in the mouse small intestine. I. Normal villi: the steady state requirement. Cell Tissue Kinet 1982;15:595–609.
7. van der Flier LG, Haegebarth A, Stange DE, et al. OLFM4 is a robust marker for stem cells in human intestine and marks a subset of colorectal cancer cells. Gastroenterology 2009;137:15–17.
8. Montgomery RK, Carlone DL, Richmond CA, et al. Mouse telomerase reverse transcriptase (mTert) expression marks slowly cycling intestinal stem cells. Proc Natl Acad Sci U S A 2011;108:179–184.
9. Pinto D, Gregorieff A, Begthel H, et al. Canonical Wnt signals are essential for homeostasis of the intestinal epithelium. Genes Dev 2003;17:1709–1713.
10. Kuhnert F, Davis CR, Wang HT, et al. Essential requirement for Wnt signaling in proliferation of adult small intestine and colon revealed by adenoviral expression of Dickkopf-1. Proc Natl Acad Sci U S A 2004;101:266–271.
11. Sato T, van Es JH, Snippert HJ, et al. Paneth cells constitute the niche for Lgr5 stem cells in intestinal crypts. Nature 2011;469:415–418.
12. Durand A, Donahue B, Peignon G, et al. Functional intestinal stem cells after Paneth cell ablation induced by the loss of transcription factor Math1 (Atoh1). Proc Natl Acad Sci U S A 2012;109:8965–8970.
13. Kim TH, Escudero S, Shivdasani RA. Intact function of Lgr5 receptor-expressing intestinal stem cells in the absence of Paneth cells. Proc Natl Acad Sci U S A 2012;109:3932–3937.
14. Garabedian EM, Roberts LJ, McNevin MS, et al. Examining the role of Paneth cells in the small intestine by lineage ablation in transgenic mice. J Biol Chem 1997;272:23729–23740.
15. Farin HF, Van Es JH, Clevers H. Redundant sources of Wnt regulate intestinal stem cells and promote formation of Paneth cells. Gastroenterology 2012;143:1518–1529 e1517.
16. Sackett SD, Fulmer JT, Friedman JR, et al. Foxl1-Cre BAC transgenic mice: a new tool for gene ablation in the gastrointestinal mesenchyme. Genesis 2007;45:518–522.
17. Guan KL, Dixon JE. Eukaryotic proteins expressed in Escherichia coli: an improved thrombin cleavage and purification procedure of fusion proteins with glutathione S-transferase. Anal Biochem 1991;192:262–267.
18. Candia AF, Wright CV. Differential localization of Mox-1 and Mox-2 proteins indicates distinct roles during development. Int J Dev Biol 1996;40:1179–1184.
19. Gregorieff A, Pinto D, Begthel H, et al. Expression pattern of Wnt signaling components in the adult intestine. Gastroenterology 2005;129:626–638.
20. Silahtaroglu AN. LNA-FISH for detection of microRNAs in frozen sections. Methods Mol Biol 2010;659:165–171.
21. Fukamachi H, Fukuda K, Suzuki M, et al. Mesenchymal transcription factor Fkh6 is essential for the development and differentiation of parietal cells. Biochem Biophys Res Commun 2001;280:1069–1076.
22. Kaestner KH, Bleckmann SC, Monaghan AP, et al. Clustered arrangement of winged helix genes fkh-6 and MFH-1: possible implications for mesoderm development. Development 1996;122:1751–1758.
23. Kaestner KH, Silberg DG, Traber PG, et al. The mesenchymal winged helix transcription factor Fkh6 is required for the control of gastrointestinal proliferation and differentiation. Genes Dev 1997;11:1583–1595.
24. Sheaffer KL, Kim R, Aoki R, et al. DNA methylation is required for the control of stem cell differentiation in the small intestine. Genes Dev 2014;28:652–664.
25. de Lau W, Peng WC, Gros P, et al. The R-spondin/Lgr5/Rnf43 module: regulator of Wnt signal strength. Genes Dev 2014;28:305–316.
26. Worthley DL, Churchill M, Compton JT, et al. Gremlin 1 identifies a skeletal stem cell with bone, cartilage, and reticular stromal potential. Cell 2015;160:269–284.

27. Perreault N, Sackett SD, Katz JP, et al. Foxl1 is a mesenchymal Modifier of Min in carcinogenesis of stomach and colon. Genes Dev 2005;19:311–315.
28. Buch T, Heppner FL, Tertilt C, et al. A Cre-inducible diphtheria toxin receptor mediates cell lineage ablation after toxin administration. Nat Methods 2005;2:419–426.
29. Saito M, Iwawaki T, Taya C, et al. Diphtheria toxin receptor-mediated conditional and targeted cell ablation in transgenic mice. Nat Biotechnol 2001;19:746–750.
30. Hoffman J, Kuhnert F, Davis CR, et al. Wnts as essential growth factors for the adult small intestine and colon. Cell Cycle 2004;3:554–557.
31. Blache P, van de Wetering M, Duluc I, et al. SOX9 is an intestine crypt transcription factor, is regulated by the Wnt pathway, and represses the CDX2 and MUC2 genes. J Cell Biol 2004;166:37–47.
32. Kabiri Z, Greicius G, Madan B, et al. Stroma provides an intestinal stem cell niche in the absence of epithelial Wnts. Development 2014;141:2206–2215.
33. San Roman AK, Jayewickreme CD, Murtaugh LC, et al. Wnt secretion from epithelial cells and subepithelial myofibroblasts is not required in the mouse intestinal stem cell niche in vivo. Stem Cell Reports 2014;2:127–134.

Received December 12, 2015. Accepted December 18, 2015.

Correspondence
Address correspondence to: Klaus H. Kaestner, PhD, Department of Genetics, Institute for Diabetes, Obesity, and Metabolism, Perelman School of Medicine, University of Pennsylvania, 12-126 Translational Research Center, 3400 Civic Center Boulevard, Philadelphia, Pennsylvania 19104. e-mail: kaestner@mail.med.upenn.edu; fax: (215) 573-5892.

Acknowledgments
The authors thank Tia Bernard-Banks for technical assistance with the mouse colony.

Conflicts of interest
The authors disclose no conflicts.

Funding
Supported by grants from the National Institutes of Health/National Institute of Diabetes and Digestive and Kidney Diseases R37-DK053839 (K.H.K.), and 5U01-DK089570 and 5U01-DK072473 (C.V.E.W.). Also supported by the Transgenic Mouse and Molecular Pathology and Imaging Cores of the Center for Molecular Studies in Digestive and Liver Diseases (National Institutes of Health P30 DK050306).